



Chemical Science

Supplementary

Phage Display Selected Magnetite Interacting Adhirones For Shape Controlled Nanoparticle Synthesis

Andrea E. Rawlings^a, Jonathan P. Bramble^a, Anna A.S. Tang^b, Lori A. Somner^a, Amy E. Monnington^c, David J. Cooke^c, Michael J. McPherson^b, Darren C. Tomlinson^b, Sarah S. Staniland^a

^aDepartment of Chemistry, The University of Sheffield, Sheffield, UK.

^bFaculty of Biological Sciences, The University of Leeds, Leeds, UK.

^cChemical and Biological Sciences, The University of Huddersfield, Huddersfield, UK.

Experimental

Preparation of nanoparticles for phage display.

A total of 5 ml 0.2M Fe(acac)₃ solution in benzyl ether was injected at 10 ml/h into a 15 ml solution of benzyl ether containing oleic acid, oleylamine and tetradecanediol at 290 °C. The solution was refluxed at 290 °C under argon for 4 h with constant stirring and then allowed to cool to room temperature. The nanoparticles were precipitated by adding anhydrous acetone and stirred for 2 h, magnetically extracted, and re-suspended in hexane containing oleic acid and oleylamine. This process was repeated five times to ensure that that unreacted iron compounds and benzyl ether were removed from the solution. The final product was stored in hexane under nitrogen in a sealed vial. A phase transfer process was used to exchange the nanoparticles into an aqueous phase¹. 5 ml of the nanoparticle solution was mixed with 5 ml of a 1.7% solution of TMAOH in degassed water and stirred for 12 h. Anhydrous acetone was added and the mixture centrifuged and the supernatant discarded. A small amount of TMAOH (25%) was added to the nanoparticles before re-suspension in water. When the particles were used for subsequent experiments, the nanoparticles were washed with degassed water three times.

Phage Display Panning

Magnetite nanoparticles were incubated with the phage library in 2x blocking buffer (BB) (Sigma) prepared in nitrogen sparged phosphate buffered saline with Tween (PBS-T) for one hour on a rotating bloodwheel. Nitrogen sparging minimises formation of alternative iron oxides on the particle surface. The particles were washed three times with fresh nitrogen sparged PBS-T to remove unbound phage. Bound phage were eluted with 0.2 M glycine pH 2.2, followed by triethylamine. The eluted phage were used to infect *E. coli* cells to amplify the phage pool and in addition the MNP particles were also mixed directly with *E. coli* cells to facilitate any further infection of bound phage. Cells were cultured and the phage isolated and used in a subsequent panning round.

Phage ELISA

Magnetite nanoparticles were mixed with 300 µl of 2 x blocking buffer (BB) (Sigma) prepared in phosphate buffered saline with tween (PBST) and supplemented with 2 µl of phage. The phage were allowed to bind to the particles over one hour with mixing, before transferring them magnetically using a KingFisher robot (Thermo) into 1 ml wash solution comprising 2 x BB PBST for 5 minutes with mixing. The particles were magnetically removed from the wash and placed into 2 x BB PBST containing rabbit Anti-fd bacteriophage (Sigma) at 1/1000 ratio for 1 hour in a final volume of 150 µl. This was followed by a washing step as before and then transferred into 150 µl of 2 x BB PBST containing Anti-Rabbit IgG alkaline phosphatase (Sigma) conjugated antibody at a 1/30,000 ratio for 1 h. Finally the particles were washed again before being introduced into 150 µl of freshly prepared BluePhos microwell reagent (KPL) for 15 minutes. The particles were then magnetically removed and the absorbance at 600 nm of each well was measured using a microplate reader.

DNA sequencing

Based on the phage ELISA results, the 48 clones which showed the highest intensity were selected and used to infect *E. coli* cells and the phagemid vectors were subsequently extracted by mini-preparation. The Adhiron coding regions were sequenced using an M13 promoter primer (Beckman Coulter Genomics) and the sequences aligned.

Protein production

The MIA-1 and 2 coding sequences, as well as the control Adhiron were amplified by PCR and introduced into pPR-IBA1 expression vectors (IBA) via conventional restriction cloning using *Bsa*I restriction sites. The resulting plasmids encode a C-terminal StrepII tag² to facilitate purification. The primers used were:

- Adhiron-IBA1f 5'-ATGGTAGGTCTCAAATGAAAAAGATTGGTTGGCTCTGGCTGGTC-3'
- Adhiron-IBA1r 5'-ATGGTAGGTCTCAGCGCTCGCGGCCGAGCGTCAC-3'.

A codon for cysteine was introduced on the end of the C-terminal tag via site-directed mutagenesis using primers:

- IBA1Cys-f 5'-CGCAGTTCGAAAAATGCTAATAAGCTTGATCC-3'
- IBA1Cys-r 5'-GGATCAAGCTTATTAGCATTTTTCGAACTGCG-3'.

The presence of the cysteine codon was confirmed by DNA sequencing. The target proteins were produced in *E. coli* BL21 (DE3) RP cells (Stratagene) using autoinduction medium (Formedium) at 37°C with vigorous shaking. The cells were harvested by centrifugation (20 minutes at 3,000 x *g*), resuspended in phosphate buffered saline (PBS) and lysed via sonication, and insoluble debris removed by centrifugation (45 minutes at 16,000 x *g*). StrepII tagged proteins were isolated from the soluble fraction by application to Streptactin resin (GE Healthcare) and elution with 2.5 mM d-Desthiobiotin dissolved in PBS. The eluate was loaded directly onto a HiTrap Heparin column (GE Healthcare) which was washed with PBS containing 500 mM NaCl. Bound Adhiron were eluted with PBS containing 750 mM NaCl and the eluate was dialysed against ultrapure water using 3.5 kDa MWCO snakeskin tubing (Thermo Scientific).

Quartz Crystal Microbalance with Dissipation. (QCM-D)

A Q-Sense E4 Quartz Crystal Microbalance with Dissipation (QCM-D) system was used to study interactions between the purified MIA, Au surfaces and magnetite nanoparticles. Gold coated QCM-D crystals were cleaned prior to use with UV ozone treatment and ethanol. The crystal resonance frequencies were stabilised in PBS buffer prior to addition of MIA at 0.1 ml/min at a typical concentration of 2.5 μM in PBS. Once stabilized, the adsorbed protein layer was rinsed in ultra-pure water and returned to PBS buffer. Magnetite nanoparticles were injected into the reaction chamber at 0.1 ml/min.

Magnetite nanoparticle synthesis with protein.

Magnetite nanoparticles were prepared using room temperature coprecipitation of mixed valence iron salts (RTCP) and by partial oxidation of ferrous hydroxide. For RTCP, a 250 mM NaOH solution was added dropwise into a solution containing Fe(II) and Fe(III) sulfate. The molar ratio of Fe (III) to total Fe was 0.3 and the ratio of hydroxide to total Fe was 4. A total iron concentration of 50 mM was used for all experiments, and confirmed by inductively coupled plasma mass spectrometry. For the high temperature reaction, 0.6 ml of a 500 mM FeSO₄ solution was added to 4.4 ml degassed ultrapure water, and 1 ml of a 500 mM KOH solution was added dropwise. This was followed by 1 ml of a 500 mM KNO₃ solution. The solution was stirred and kept under nitrogen and heated to 90 °C for 3 h. Nitrogen sparged ultrapure water was used for all nanoparticle synthesis and precipitations were carried out in oxygen free conditions. After completion of each reaction, the black magnetite precipitate was washed three times in degassed water and stored under nitrogen. Chemicals were purchased from Sigma-Aldrich. Protein was added to a concentration of 50 μg per 10 ml reaction solution, consistent with previous studies of biomineralisation *in vitro*^{3, 4}. 5 and 500 μg were also screened. Peptides of MIA-1 loops (Genscript) were dissolved in ultrapure water to a concentration of 1 mg/ml and dialysed overnight against ultrapure water using 1 kDa MW cut off dialysis cassettes (GE Healthcare) to remove any residual salts. 4 μl of each dialysed peptide was added to 10 ml of precipitation reaction.

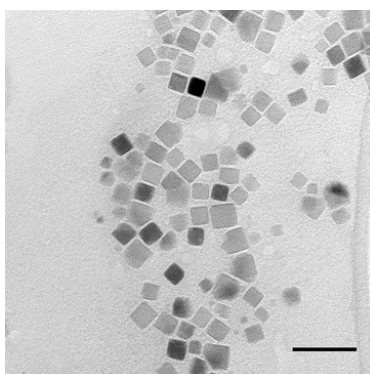
Nanoparticle characterisation.

Nanoparticles were visualised using an FEI Technai G2 Spirit TEM. Size analysis was performed with ImageJ. HRTEM images were collected on a Phillips CM200 and analysed with ImageJ and SingleCrystal. Powder X-ray diffraction was carried out on nanoparticle samples which were dried *in vacuo*. The samples were rotated from 5-80° and the resulting diffraction peaks analysed. For the nanoparticle ELISA, 500 μg of magnetite or zinc oxide nanoparticles (NP) were blocked with 2 x blocking buffer in PBS-T. 1 μg of Adhiron was added to each sample with binding for 1 hour. NP were washed with PBS-T prior to addition of rabbit anti-StrepII antibody (Promokine) for 1 hour. NP were washed again, and Anti-Rabbit IgG alkaline phosphatase added. After 1 hour the NP were washed with PBS-T and detected with Blue-Phos reagent. After 15 minutes the particles were magnetically removed and the absorbance of the supernatant at 600 nm recorded.

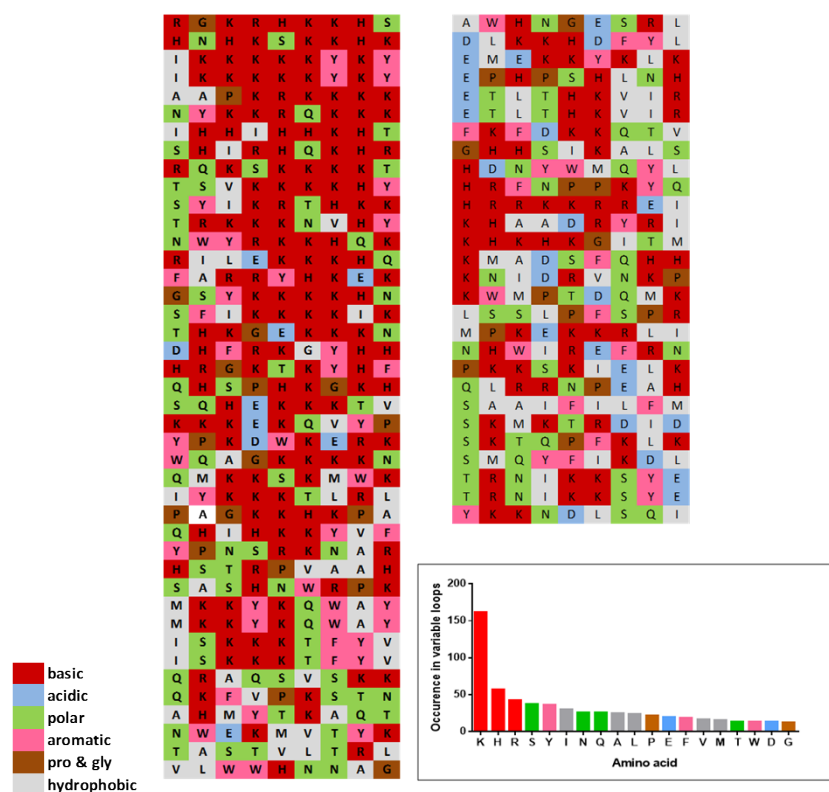
MD simulations.

Molecular dynamics simulations were performed using the DL_POLY classic code⁵ where the short-range inter and intra-molecular interactions were described using the AMBER force field ff99SB6 for the organic molecules, a modified version of CLAYFF for magnetite^{6,7} and TIP3P/Fs⁸ for water. The structures of the five amino acids were generated using the AMBERTOOLS package TLEAP⁹. The sequences were capped, using the ACE and NME method thus neutralising the C- and N-terminal charges and more accurately replicating conditions within a peptide chain. The adsorption energy of the molecule was then determined by comparing the energy of a system containing a magnetite slab and adsorbed amino acid to the energy of an isolated amino acid molecule. A complete description of the computational methodology is available in supplementary method.

Supplementary information.



Supplementary fig. 1: Magnetite nanoparticles for phage display. TEM image of cubic magnetite nanoparticles created in a hot-injection process for phage selection. Scale bar 50nm.



Supplementary fig. 2: Binding loop sequence analysis. The sequences of the variable binding loops are shown, coloured by amino acid type. The frequency with which each residue is selected is depicted in the plot, coloured to correspond to the sequence data.

Calculation of theoretical Adhiron coverage of nanoparticles.

- Estimating the concentration of magnetite nanoparticle produced in a typical 10 ml magnetite coprecipitation reaction. Average size of particles is 30 nm. Assuming a predominantly cube morphology.

Volume per particle: $30 \text{ nm} \times 30 \text{ nm} \times 30 \text{ nm} = 27,000 \text{ nm}^3 = 2.7 \times 10^{-17} \text{ cm}^3$

Density of Magnetite: 5 g cm^{-3}

Mass per particle (assuming all are magnetite): $5 \text{ g} / 2.7 \times 10^{-17} \text{ cm}^3 = 1.35 \times 10^{-16} \text{ g}$

Moles of iron in 10 ml coprecipitation = $500 \text{ } \mu\text{mol}$

$500 \text{ } \mu\text{mol} / 3 = 166.7 \text{ } \mu\text{mol}$ of Fe_3O_4 .

MW of magnetite is $231.54 \text{ g mol}^{-1}$

Mass of magnetite (assuming full conversion): $166.7 \times 10^{-6} \times 231.54 = 0.0385 \text{ g}$

Number of particles: $0.0385 \text{ g} / 1.35 \times 10^{-16} \text{ g} = 2.85 \times 10^{14}$

Concentration of particles: $2.85 \times 10^{14} / 6.02 \times 10^{23} = 4.73 \times 10^{-10} \text{ M} = 0.47 \text{ nM}$

- Estimating the surface area of a nanoparticle. Assuming 30 nm cubic nanoparticles.

Surface area of a particle: $(30 \text{ nm} \times 30 \text{ nm}) \times 6 = 5400 \text{ nm}^2$

- Estimating the surface area of the binding region of the Adhiron. Based on available crystal structure (PDB: 4N6T).

$3.2 \text{ nm} \times 2.1 \text{ nm} = 6.7 \text{ nm}^2$

- Theoretical number of proteins to achieve a monolayer coverage of a single nanoparticle (assuming close packing). $5400 \text{ nm}^2 / 6.7 \text{ nm}^2 = 803$ Adhiron per particle.

Table 1: Estimated Adhiron per magnetite nanoparticle.

Mass of MIA / μg^*	Concentration MIA / nm	Estimated Adhiron per MNP [†]	Ratio of MIA to MIA monolayer MNP
5	33	69	0.086
50	333	697	0.86
500	3333	6976	8.6

*Mass of Adhiron added to a 10 ml magnetite coprecipitation. [†] Calculated by dividing the concentration of Adhiron by the estimated concentration of particles.

From this estimate of Adhiron per particle we see that addition of 50 μg to each 10 ml coprecipitation provides sufficient Adhiron to control the formation of all theoretical cube planes of the nanoparticle products. At 5 μg we are adding a suboptimal amount of Adhiron- which matches the TEM results showing no apparent effect on particle morphology. The 500 μg addition provides an approximate 10 fold excess of Adhiron which appears to hamper the magnetite reaction, resulting in heterogeneous particle morphologies.

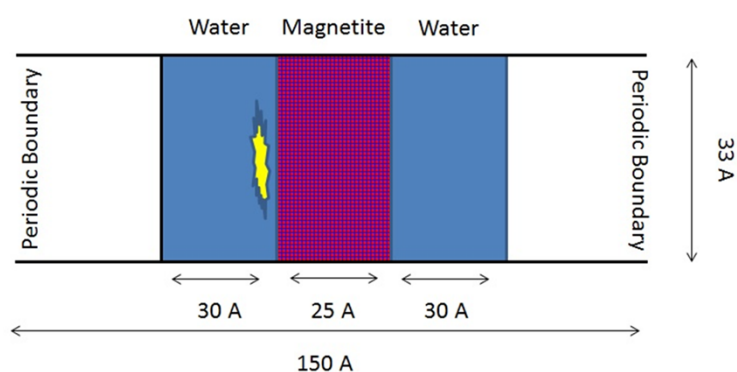
Details of the theoretical methods employed.

The DL_POLY Classic code¹⁰ was used to perform the molecular dynamic simulations using the NVT (constant number of particles, volume and temperature) ensemble, employing the Nosé-Hoover thermostat¹¹ with a relaxation time of 0.5 ps. The trajectories were generated using the Verlet leapfrog algorithm¹² using a time step of 1.0 fs. The long-range Coulombic interactions were calculated using Ewald summation¹³ and the short-range inter and intra-molecular interactions were described using the AMBER force field ff99SB¹⁴ for the organic molecules, a modified version of CLAYFF for magnetite⁶ and TIP3P/Fs⁷ for water.

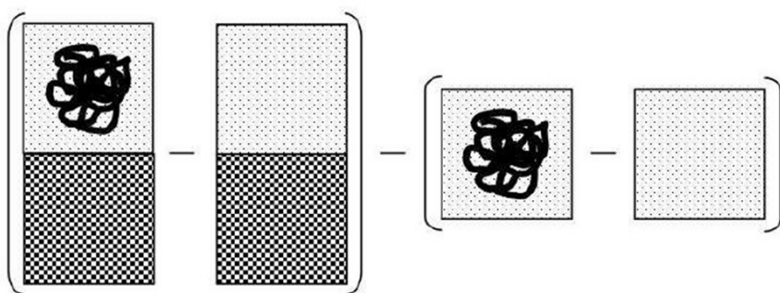
The structures of the five amino acids chosen for study, representing a mixture of basic, acidic and neutral molecules (LYS, ARG, ASP, GLU and LEU), were generated using the AMBERTOOLS package TLEAP⁹ and the molecules were capped, using the ACE and NME method⁷ thus neutralising the C- and N-terminal charges and more accurately replicating conditions within the a larger peptide chain. This system was then relaxed in vacu, using for 1 ns at 300 K in a simulation cell of dimensions 40 Å x 40 Å x 40Å. 2007 water molecules were then added to the simulation using the utility distributed with DL_POLY classic and a further 1 ns of NPT MD was performed, this allowed the size of the simulation cell to relax to reflect the true density of the system whilst simplifying the calculation of the adsorption energy as the number of water molecules in each system was constant.

A Magnetite slab terminated with the [100] surfaces perpendicular to the x-axis and approximately 25 Å thick was generated from the pre-relaxed bull structure using the METADISE (Minimum Energy Techniques Applied to Dislocation, Interface and Surface Energies) code⁸. The relaxed amino-acid was then placed in the vacuum gap so all the atoms were at least 5 Å above the slab surface and a short (100 ps) MD simulation was performed to allow the molecule to adsorb onto the slab surface. 1125 water molecules were then added in the 30 Å. To ensure the water remained at the correct density above each of the slab surface during the simulations the x-dimension of the unit cell increased so there was a 60 Å vacuum gap above the two water layers, thus providing a void for the system to expand into or contract from, without effecting the dimensions of the magnetite slab and the nature of the adsorption layer. A schematic of the simulation setup is shown in supplementary fig. 3. Prior to the production runs, 1 ns of MD simulation was performed to allow the water and the amino acid to relax.

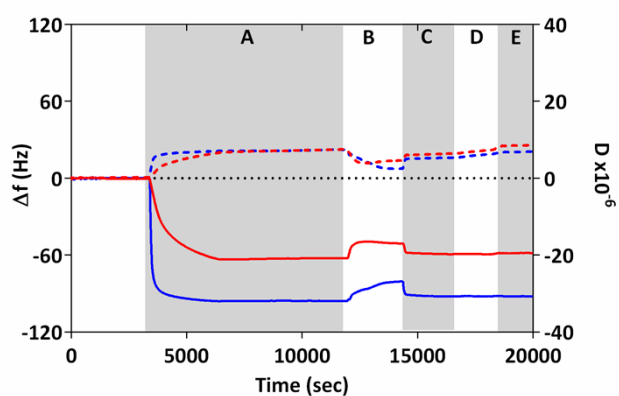
We have defined the adsorption energy of the amino acid onto the magnetite surface in the presence of water using the approach previously adopted by Harding and co-workers when studying adsorption onto calcite surfaces¹⁰ where the difference in energy of a magnetite slab with an adsorbed molecule and the energy of a the same slab with the molecule infinitely separated from it using four separate simulation cells as illustrated in supplementary fig. 4. As care was taken to insure that all the simulations containing the isolated molecule contained the same number of water molecules, and all the slab simulations were the same dimensions and contained the same number magnetite units and water molecules, these components cancel, thereby leaving the energy change associated with the molecule being brought into contact with the surface. The values used in these calculations are the average from production simulations of 5 ns, performed after the equilibrium steps described above were complete.



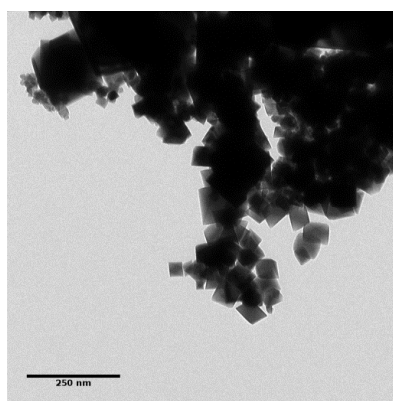
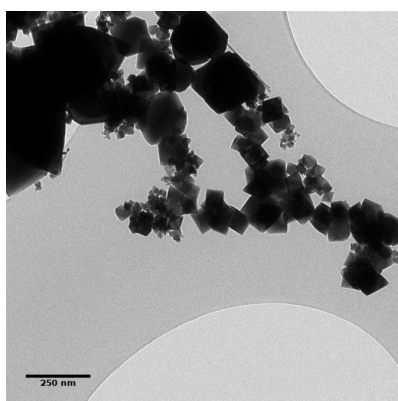
Supplementary fig. 3: Simulation set-up schematic. The simulation used periodic boundary conditions in three dimensions. The repeat distance in the plane perpendicular to the screen was 33 Å.



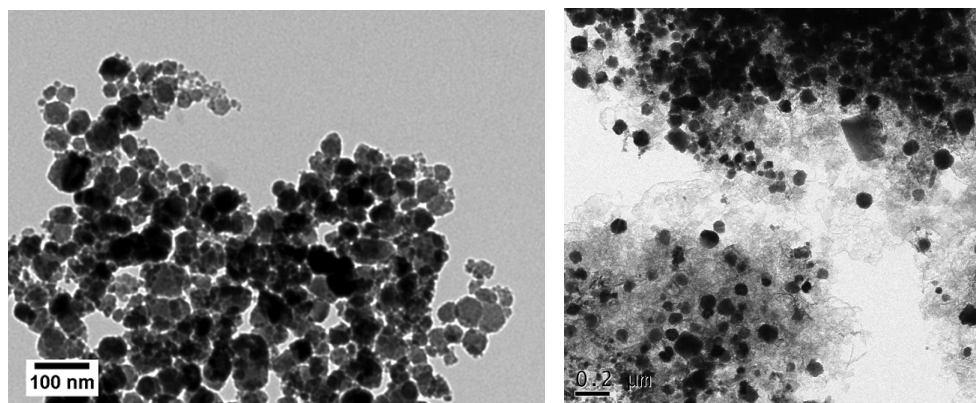
Supplementary fig. 4: Energy of adsorption calculation. A schematic representation showing the four stages needed to calculate the energy of adsorption.



Supplementary fig. 5: QCM analysis of DNA loaded MIA-1 with magnetite nanoparticles. Change in frequency, Δf , and Dissipation, D . Dotted lines represent dissipation and solid lines frequency. Red lines are DNA loaded MIA-1 and blue lines control Adhiron. Phase A is injection of protein into the system, B and C are rinses with ultrapure water and PBS respectively. MNP are injected into the system during D, and Phase E is final rinsing with PBS. No change in Δf is observed during MNP application for either sample.



Supplementary fig. 6: Partial oxidation ferrous hydroxide reaction products. TEM analysis of MNP formed by POFH with (left) MIA-1 and (right) no protein shows any significant differences in product morphology.



Supplementary fig. 7: TEM analysis of room temperature coprecipitation reaction products produced with Control Adhiron (left) and MIA-1 peptides (right).

Supplementary references.

1. E. Taboada, E. Rodríguez, A. Roig, J. Oró, A. Roch and R. N. Muller, *Langmuir*, 2007, **23**, 4583-4588.
2. T. G. Schmidt, J. Koepke, R. Frank and A. Skerra, *J Mol Biol*, 1996, **255**, 753-766.
3. A. Arakaki, J. Webb and T. Matsunaga, *J Biol Chem*, 2003, **278**, 8745-8750.
4. Y. Amemiya, A. Arakaki, S. S. Staniland, T. Tanaka and T. Matsunaga, *Biomaterials*, 2007, **28**, 5381-5389.
5. W. Smith and T. R. Forester, *Journal of molecular graphics*, 1996, **14**, 136-141.
6. R. T. Cygan, J. J. Liang and A. G. Kalinichev, *J Phys Chem B*, 2004, **108**, 1255-1266.
7. S. Kerisit, *Geochim Cosmochim Acta*, 2011, **75**, 2043-2061.
8. U. W. Schmitt and G. A. Voth, *J Chem Phys*, 1999, **111**, 9361-9381.
9. D. A. Case, T.A. Darden, I. T.E. Cheatham, C.L. Simmerling, J. Wang, R.E. Duke, R. Luo, R.C. Walker, W. Zhang, K.M. Merz, B. Roberts, B. Wang, S. Hayik, A. Roitberg, G. Seabra, I. Kolossváry, K.F. Wong, F. Paesani, J. Vanicek, J. Liu, X. Wu, S.R. Brozell, T. Steinbrecher, H. Gohlke, Q. Cai, X. Ye, J. Wang, M.-J. Hsieh, G. Cui, D.R. Roe, D.H. Mathews, M.G. Seetin, C. Sagui, V. Babin, T. Luchko, S. Gusarov, A. Kovalenko and P. A. Kollman, *University of California, San Francisco*, 2010.
10. W. Smith and T. R. Forester, *Journal of molecular graphics*, 1996, **14**, 136-141.
11. W. G. Hoover, *Physical review. A*, 1985, **31**, 1695-1697.
12. L. Verlet, *Phys Rev*, 1967, **159**, 98-&.
13. P. P. Ewald, *Ann Phys-Berlin*, 1921, **64**, 253-287.
14. W. D. Cornell, P. Cieplak, C. I. Bayly, I. R. Gould, K. M. Merz, D. M. Ferguson, D. C. Spellmeyer, T. Fox, J. W. Caldwell and P. A. Kollman, *Journal of the American Chemical Society*, 1995, **117**, 5179-5197.